

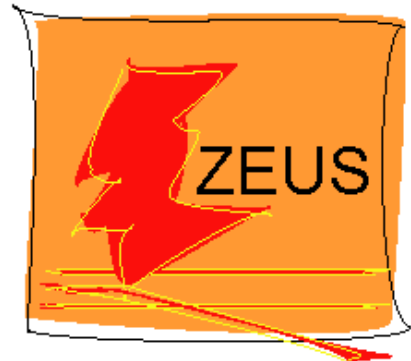


# Charm Production in CC DIS at HERA

(DESY-19-054, arXiv:1904.03261)

Jae D. Nam

Temple Univ. & ZEUS

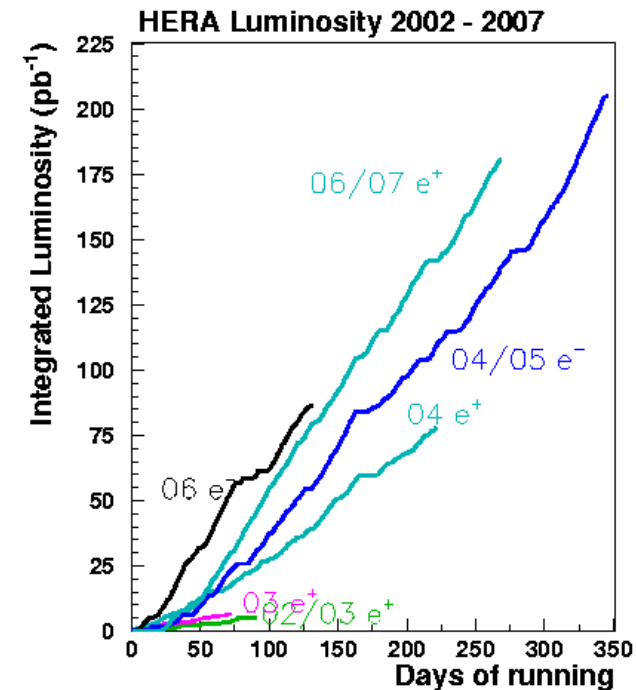
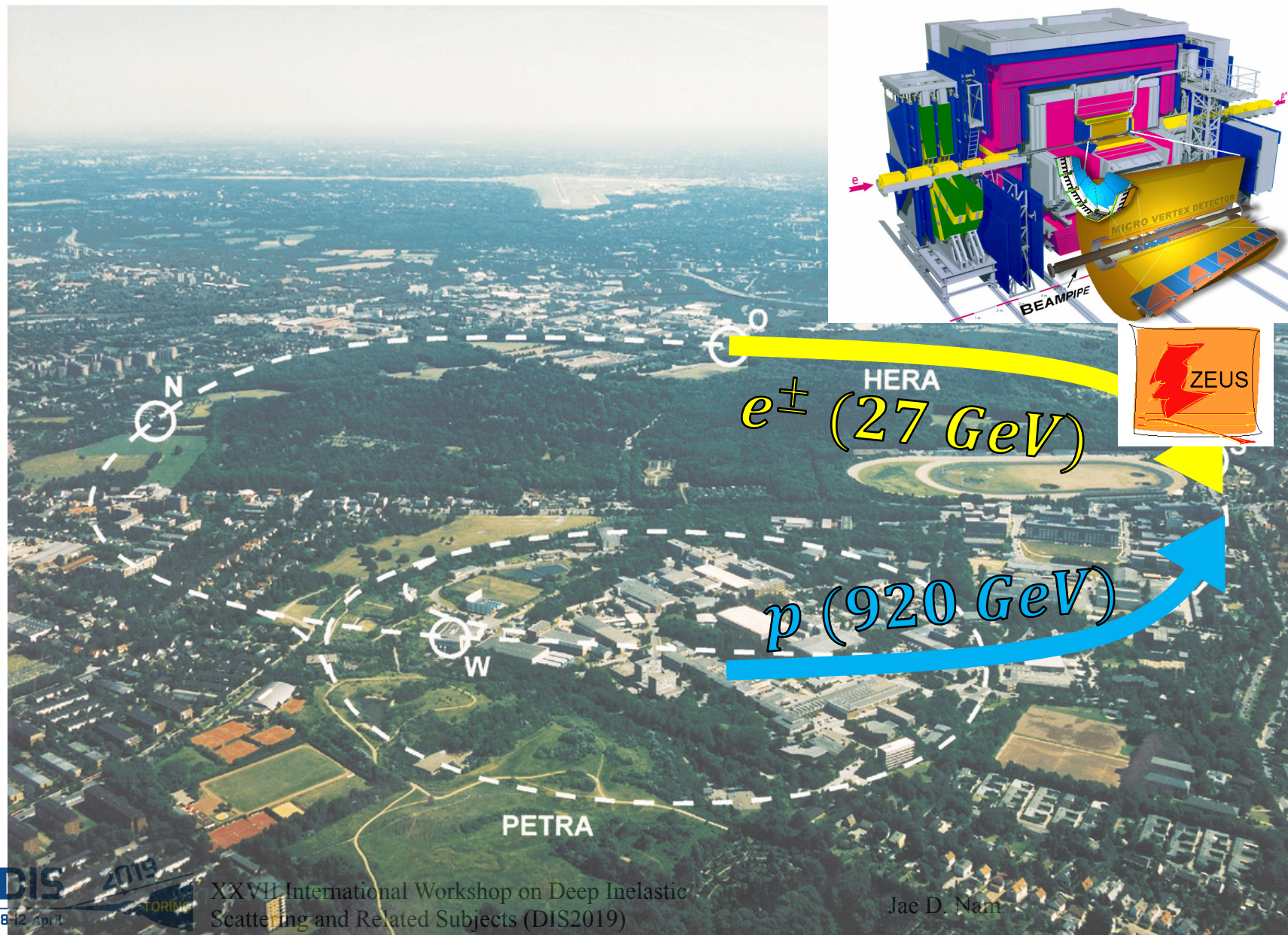


U.S. DEPARTMENT OF  
**ENERGY**

DOE NP contract: DE-SC0013405



# Hadron-Electron Ring Accelerator

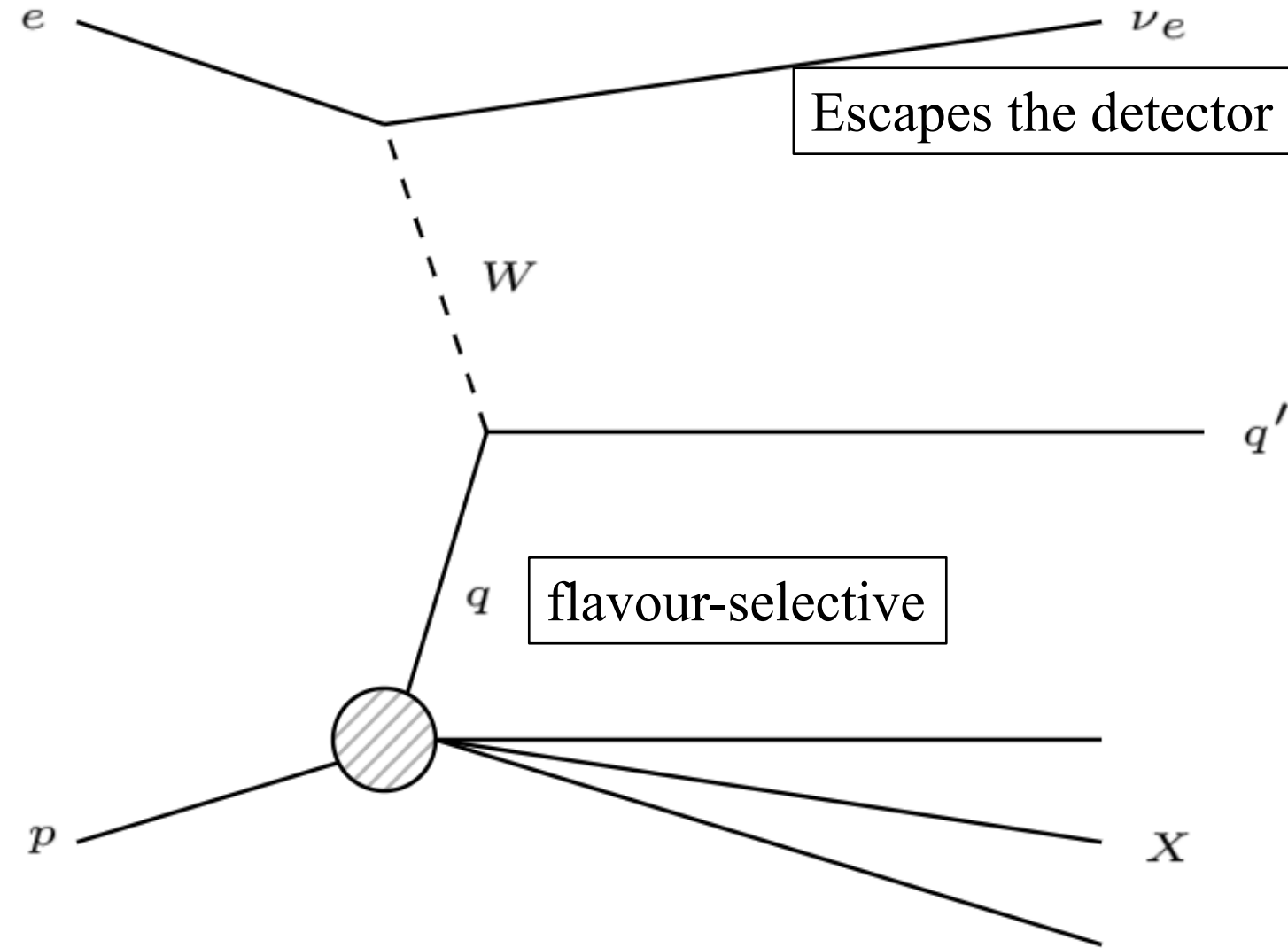


## HERA upgrade

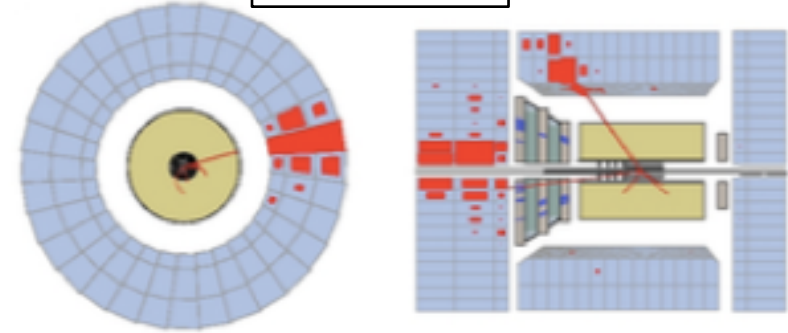
- Luminosity upgrade.
  - HERA I :  $120 \text{ pb}^{-1}$
  - HERA II :  $360 \text{ pb}^{-1}$
- Higher particle tagging capabilities through MVD & STT.



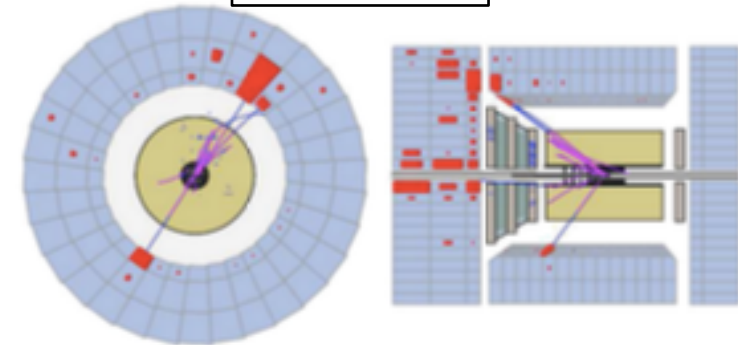
# Charged Current (CC) DIS at HERA



CC DIS



NC DIS

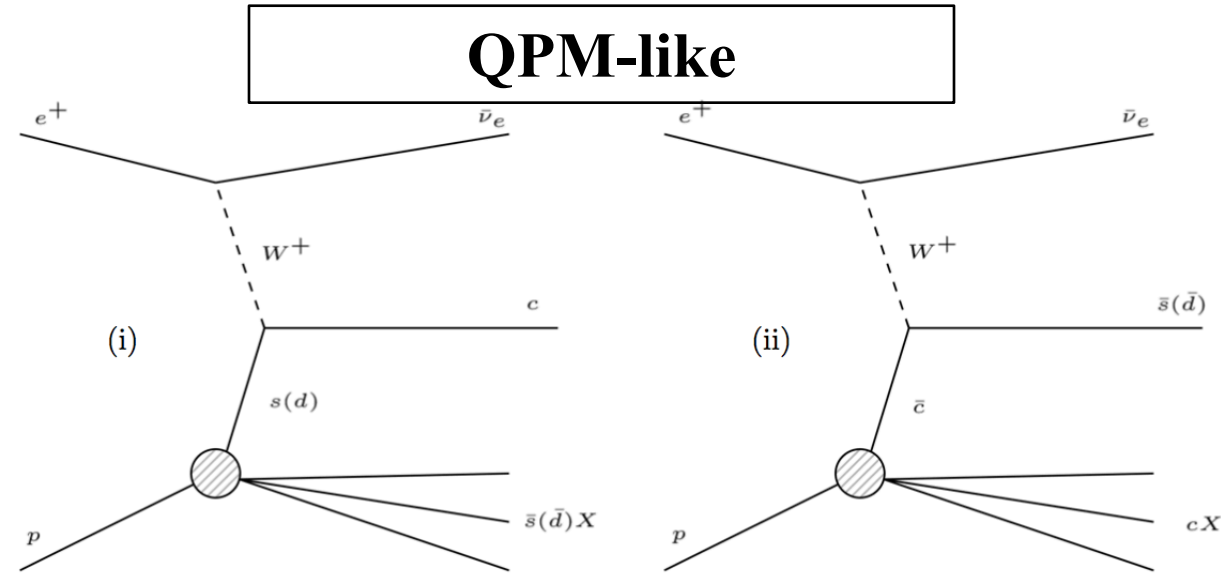


- Large missing  $p_T$  due to neutrino.
- Powerful probe of flavour-specific PDFs.
- Low production rate.



# Charm production in CCDIS

## QPM-like

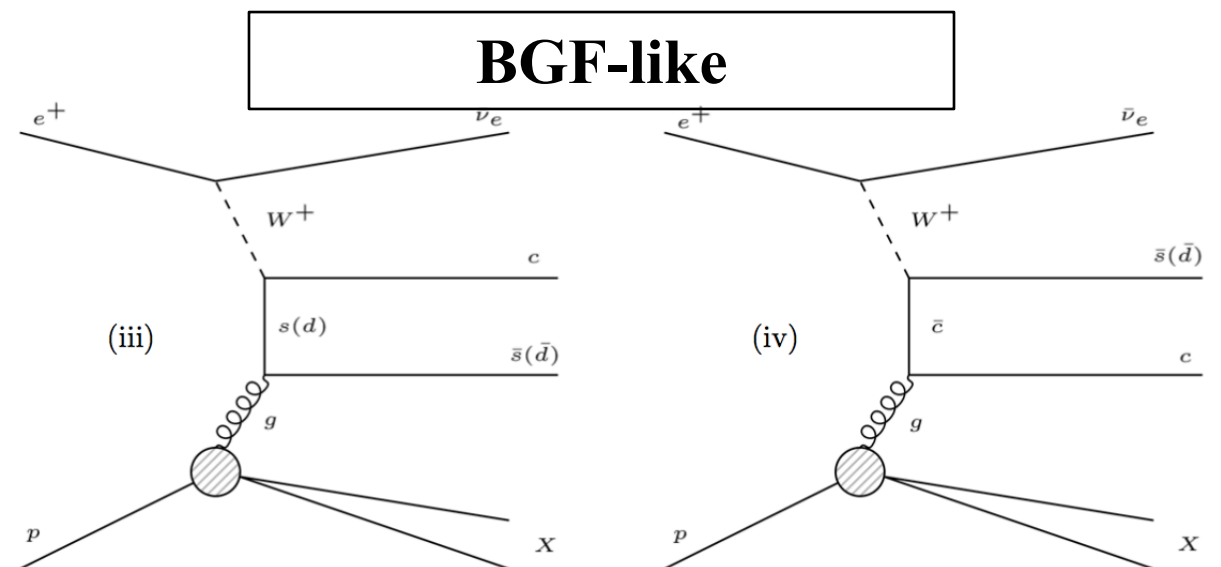


- Charm production processes in  $e^+p$  CCDIS

$$\text{QPM-like} \begin{cases} i. & s\bar{s}(d\bar{d})W^+ \rightarrow c\bar{s}(\bar{d}) \\ ii. & c\bar{c}W^+ \rightarrow c\bar{s}(\bar{d}) \end{cases}$$

$$\text{BGF-like} \begin{cases} iii. & g \rightarrow s\bar{s}(d\bar{d}) \\ iv. & g \rightarrow c\bar{c} \end{cases}$$

## BGF-like



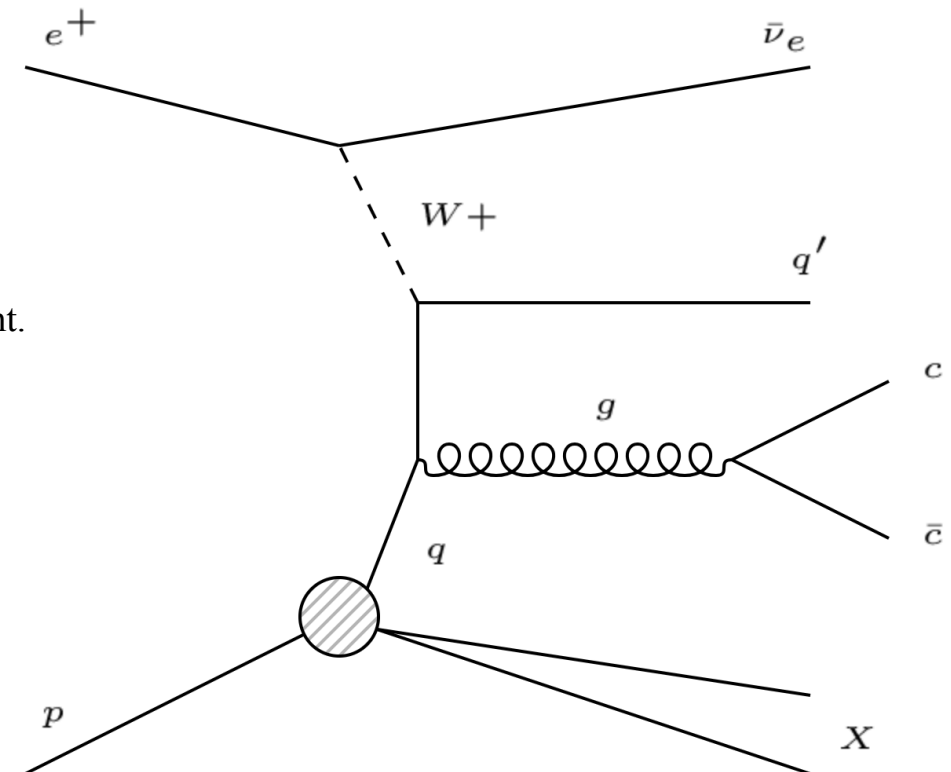
- Subprocess (i) is directly sensitive to the strangeness of the proton.
- However, the distinction of these processes depends on the choice of QCD scheme.
  - Extraction of  $s(x, Q^2)$  is model dependent.

# Motivations

- Charm in CCDIS with high- $Q^2$  HERA  $e^\pm p$  collision data collected at ZEUS.
  - Probe strangeness in the proton by measuring EW part of inclusive charm cross section in CCDIS.
  - Charm quark from final-state QCD radiation is indistinguishable due to lack of charm charge measurement & low statistics.

- Theory predictions

- Zero-mass variable-flavour-number scheme (ZM-VFNS)
  - QCDNUM, HERAPDF2.0 & ATLAS  $epWZ16$  PDF sets.
  - Used for relative comparison of different assumptions on the strange content.
- Fixed-flavour number scheme (FFN)
  - No charm quark content in the proton & larger gluon content.
  - OPENQCDRAD, ABMP16.3 NLO PDF sets.
- General-mass VFN scheme (GM-VFNS)
  - FONLL-B scheme.
  - APFEL, NNPDF3.1 sets.



# Strangeness in the proton

- Mass-suppressed strangeness :

$$f_s \left( \equiv \frac{s}{s+\bar{d}} \right) \sim 0.3$$

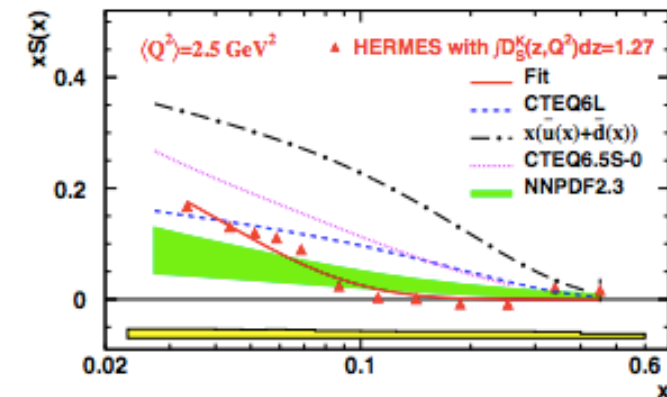
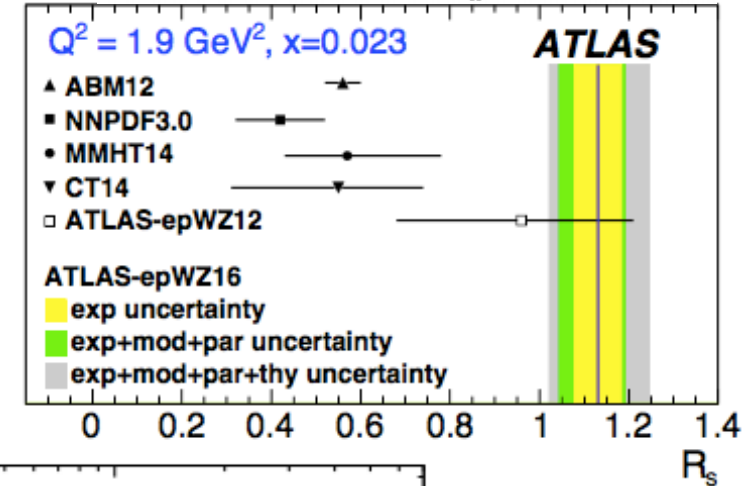
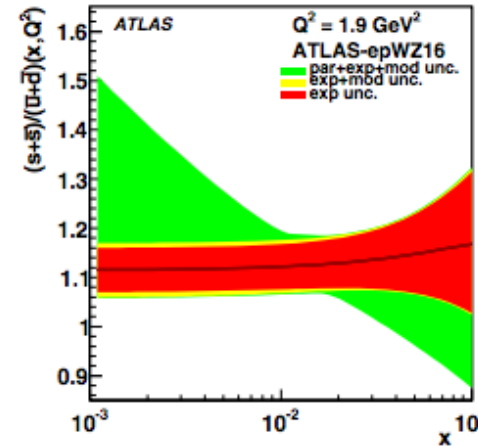
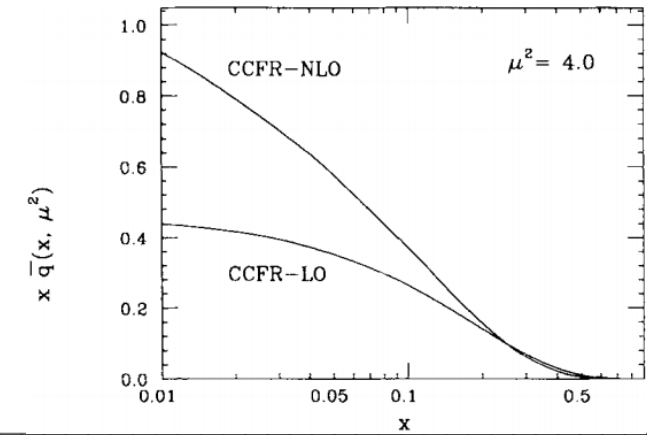
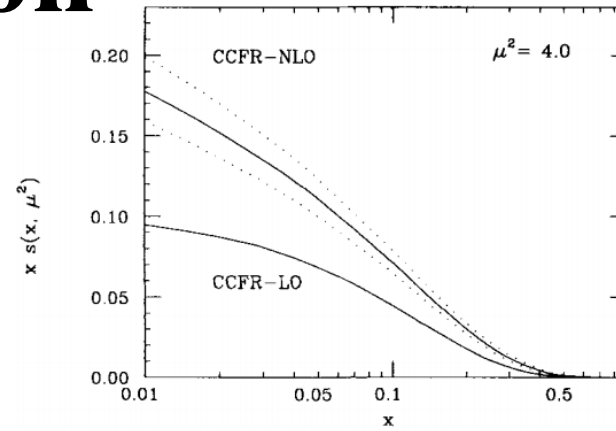
- For large  $x_{Bj}$ , experimentally supported by neutrino-scattering experiments (CCFR/NuTeV, NOMAD, CHORUS).

- Unsuppressed strangeness :  $f_s \sim 0.5$

- For small  $x_{Bj}$ , experimentally supported by high-precision  $W/Z$  production measurement (ATLAS) &  $W + c$  data (CMS).

- $x$ -dependent strangeness

- As suggested by HERMES
- $x\bar{s} = f'_s 0.5 \tanh(-20(x - 0.07)) x\bar{d}$



# DATA & MC

## Data

- HERA II ( $L \cong 360 \text{ pb}^{-1}$ )
  - $e^-p : L \cong 185 \text{ pb}^{-1}$
  - $e^+p : L \cong 173 \text{ pb}^{-1}$

Year	Collision	Integrated Luminosity ( $\text{pb}^{-1}$ )
2003/04	$e^+p$	$\sim 38$
2004/05	$e^-p$	$\sim 133$
2006	$e^-p$	$\sim 52$
2006/07	$e^+p$	$\sim 135$

- Kinematic variables ( $x, y, Q^2$ ) defined by using Jacquet-Blondel Method.

$$y_{JB} = \frac{\sum_h (E - p_z)_h}{2E_{e,beam}} \quad Q_{JB}^2 = \frac{p_{T,h}^2}{1 - y_{JB}} \quad x_{JB} = \frac{Q_{JB}^2}{s y_{JB}}$$

Jae D. Nam

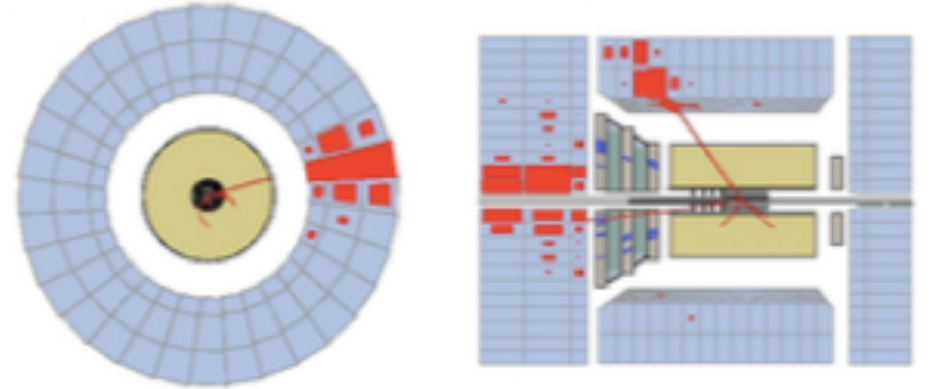
## MC

- DIS
  - Inclusive CCDIS MC, DJANGO 1.6, ARIADNE 4.12, CTEQ-5D.
- Background
  - Inclusive NCDIS MC: DJANGO 1.6, ARIADNE 4.12, CTEQ-5D
  - Photoproduction MC: HERWIG, resolved & direct
  - Background contribution was found to be negligible.
- The kinematic variables ( $x, y, Q^2$ ) obtained from the lepton information.

$$Q^2 = -(k - k')^2 \quad x = \frac{Q^2}{2pq} \quad y = \frac{pq}{pk}$$

# DIS selection

- CCDIS selection based on  $p_{T,miss}$ 
  - $p_{T,miss} > 12 \text{ GeV}$
  - $p'_{T,miss} > 10 \text{ GeV}$  (excl. cells adjacent to beam pipe)
- Non-CC DIS rejection (arXiv:1008.3493)
- Non- $ep$  background (beam-gas, beam-halo muon, cosmic) rejection
- Kinematic selection cut
  - $200 < Q^2 < 60000 \text{ GeV}^2$
  - $y < 0.9$
  - For optimal detector resolution & low background.
  - Full kinematic range of the measurement

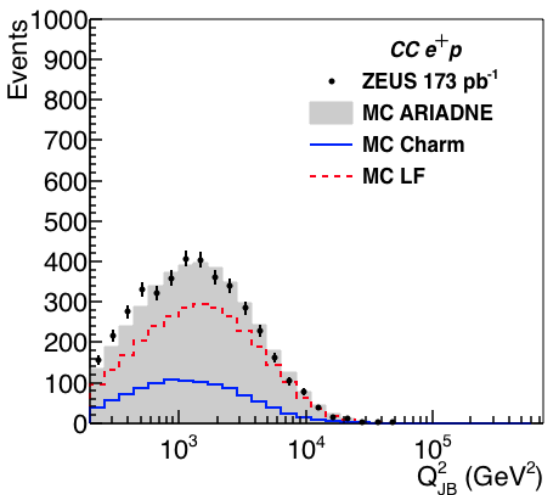




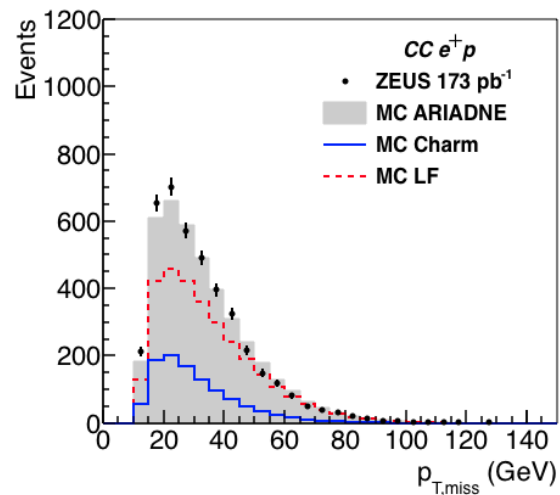
# DIS control plots

$e^+p$  collisions

ZEUS

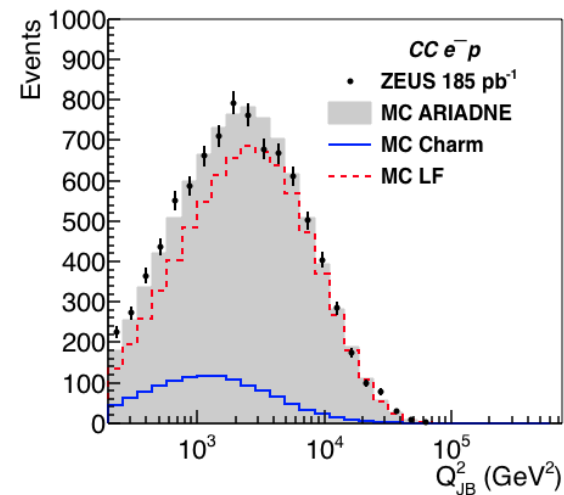


ZEUS

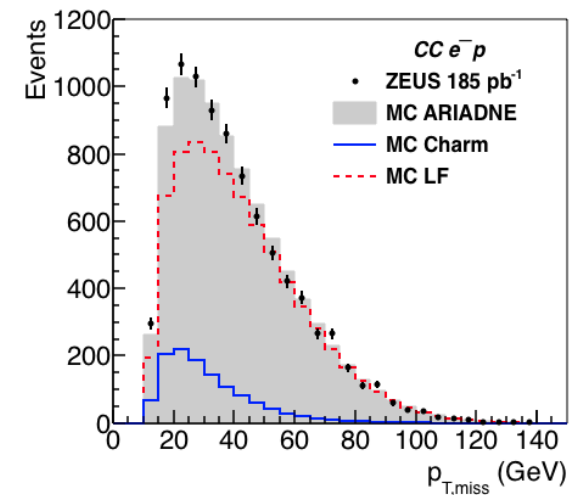


$e^-p$  collisions

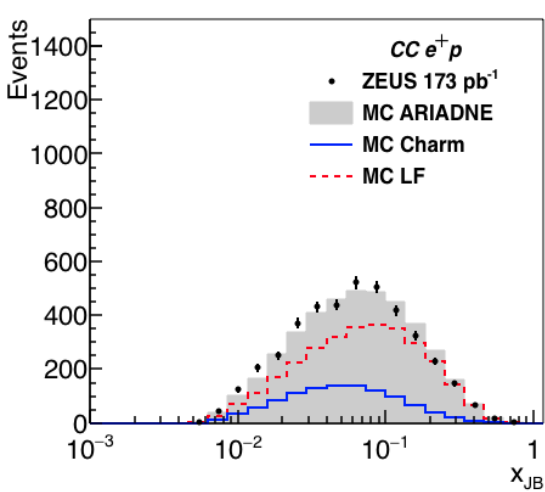
ZEUS



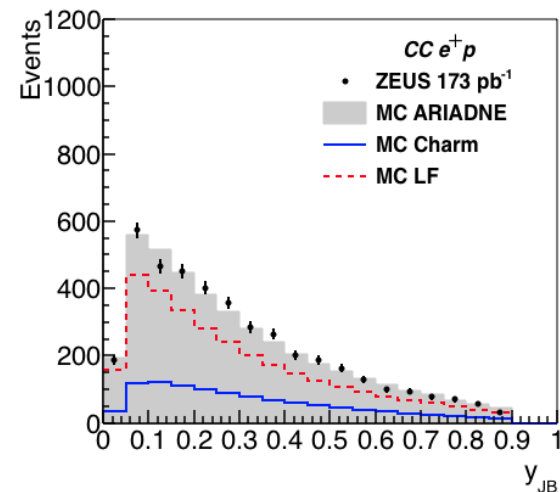
ZEUS



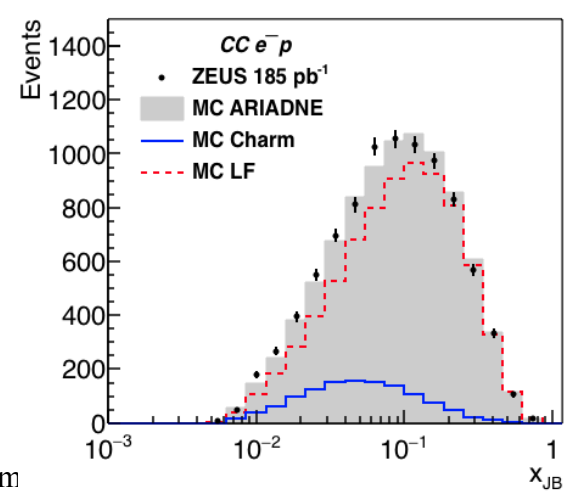
ZEUS



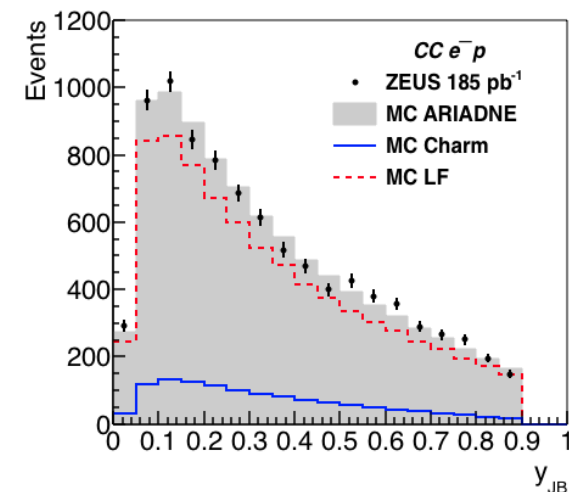
ZEUS



ZEUS



ZEUS

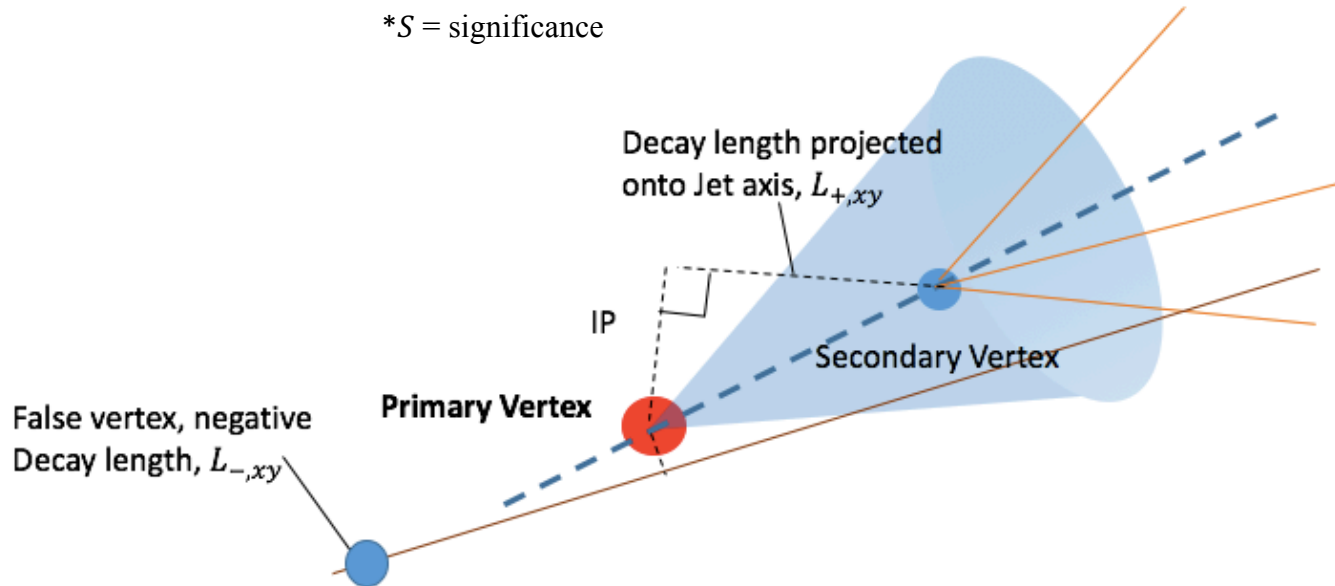


# Charm identification

## Lifetime-tagging Method

- 2D decay length ( $L_{xy}$ ) projected onto Jet axis.
  - LF  $\rightarrow$  Prompt, Symmetric decay length dist.
  - Charm  $\rightarrow$  Weakly-decaying, Asymmetric dist.
- LF contribution (background) suppressed by mirroring decay length distribution about  $L_{xy} = 0$ .  
 $(L_+ - L_-, S_+ - S_-)$

\*S = significance

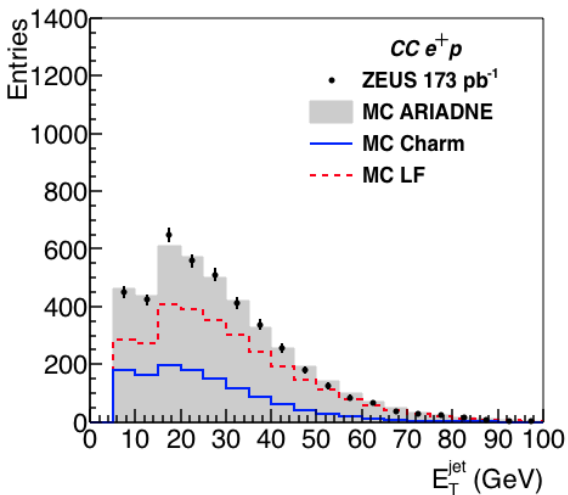


Jet Selection	Reconstructed by using $k_T$ -cluster algorithm in the massive mode.
	$E_T^{jet} > 5 \text{ GeV}$
	$-2.5 < \eta^{jet} < 2.0$ (1.5 for 05e)
	<b>Defines “visible” kinematic region.</b>
SecVtx Selection	$\chi^2/N_{dof} < 6$
	$ Z_{secvtx}  < 30 \text{ cm}$
	Distance to beam spot $\sqrt{\Delta x^2 + \Delta y^2} < 1 \text{ cm}$
	$M_{secvtx} < 6 \text{ GeV}$
	$N_{secvtx}^{trk} > 2$

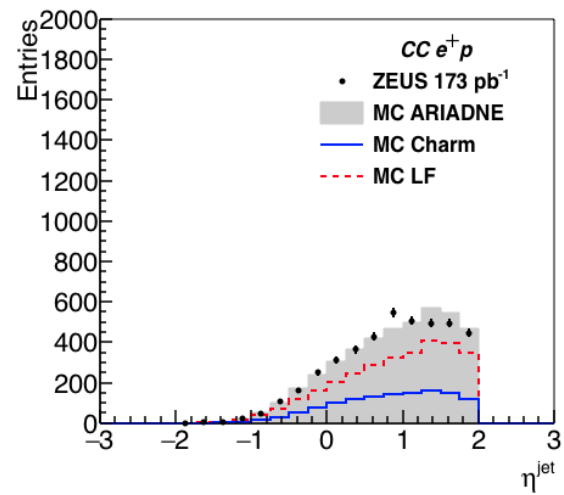
# Jet & Secondary vertex

$e^+p$  collisions

ZEUS

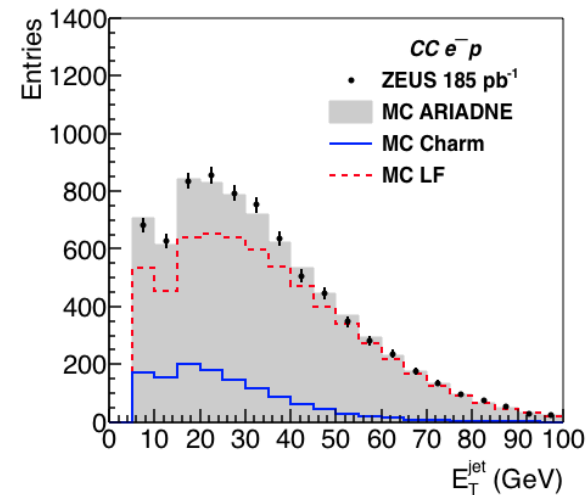


ZEUS

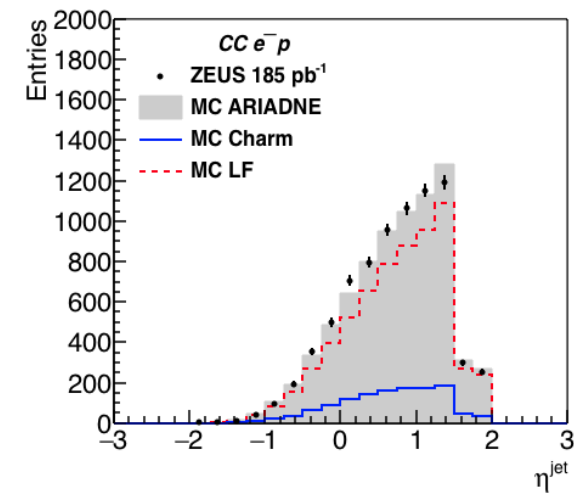


$e^-p$  collisions

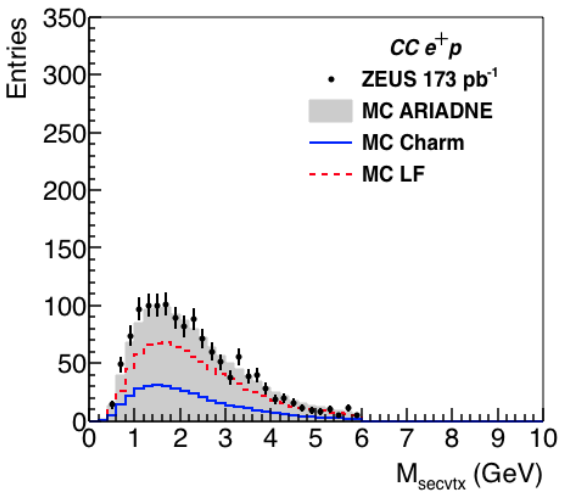
ZEUS



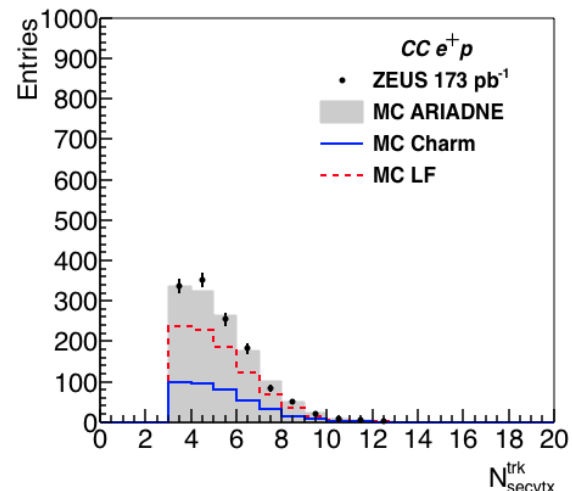
ZEUS



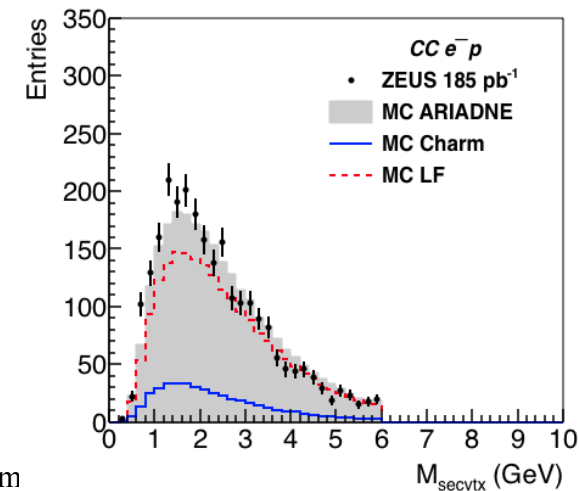
ZEUS



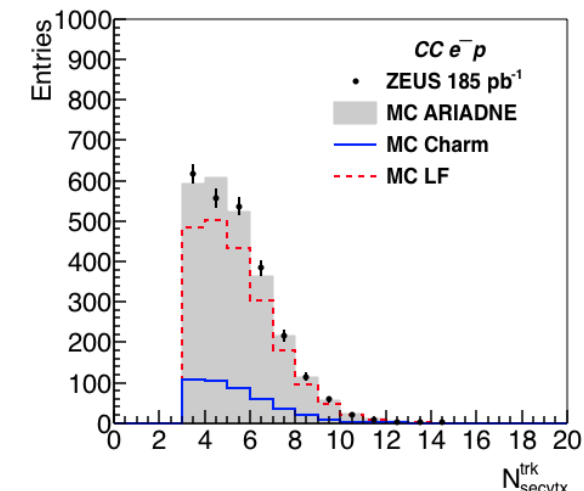
ZEUS



ZEUS



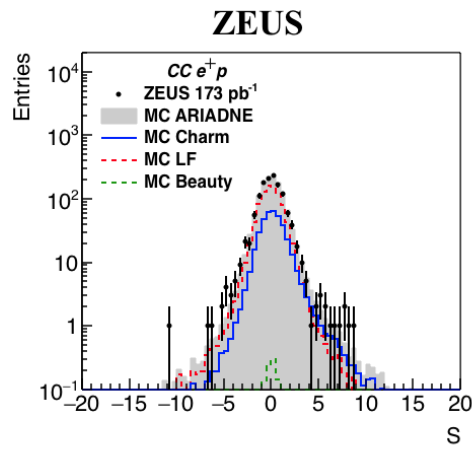
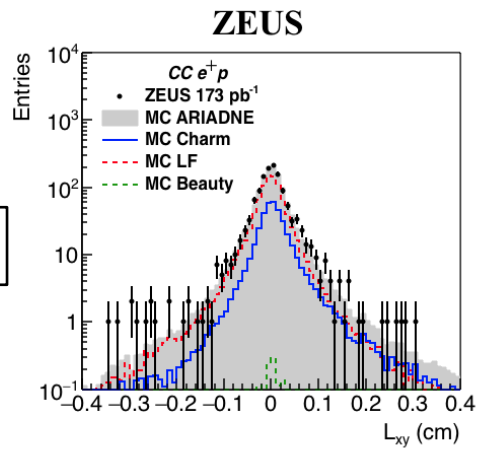
ZEUS



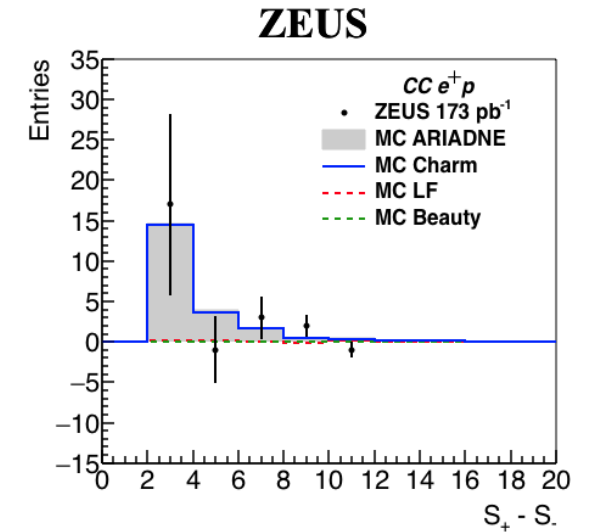
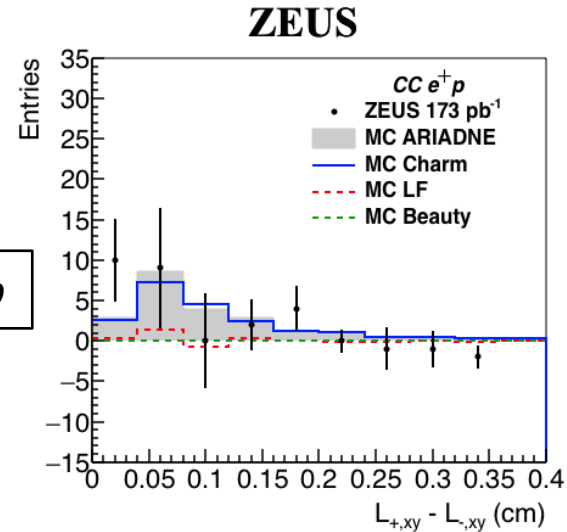
# Decay length

- Asymmetric charm distribution observed.
- Significance cut,  $S > 2$ , to improve statistical uncertainty.

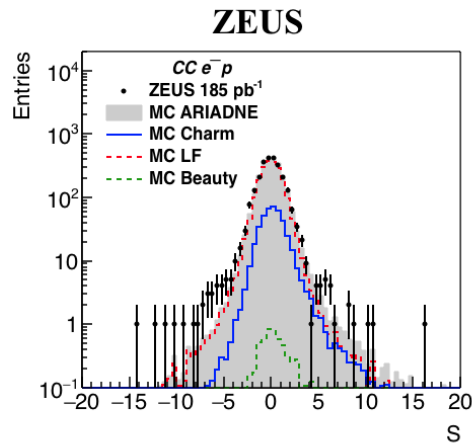
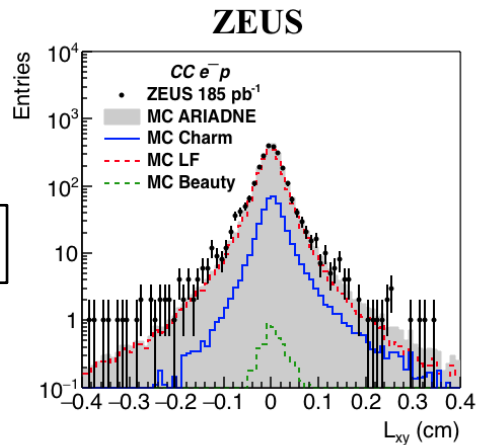
$e^+p$



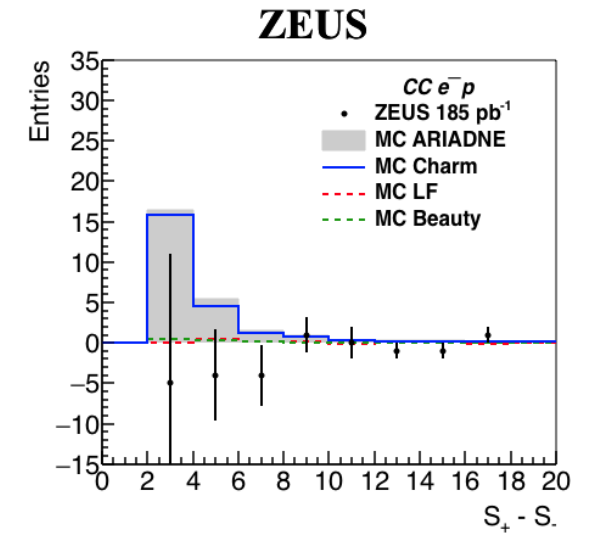
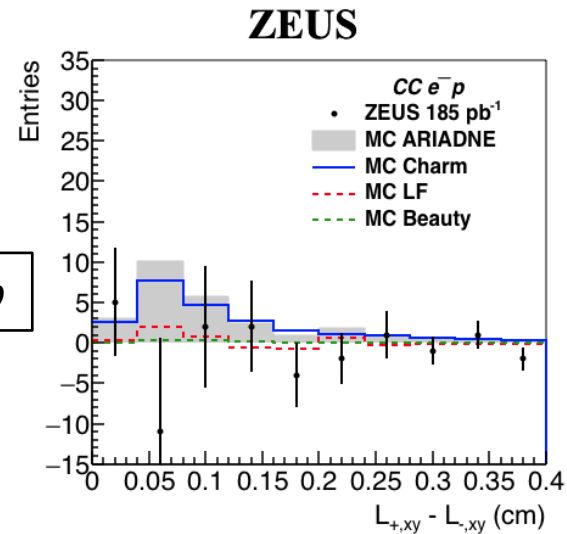
$e^+p$



$e^-p$



$e^-p$





# Charm cross section

- Visible charm cross section

$$\sigma_{c,vis} = \frac{N^{data} - N_{bg}^{MC}}{N_c^{MC}} * \sigma_c^{MC}$$

$$= \frac{N^{data} - N_{bg}^{MC}}{N_c^{MC}} * \frac{N_{vis}}{L}$$

- Visible EW charm cross section is taken from subtracting the QCD part.

$$\sigma_{c^{EW},vis} = \sigma_{c,vis} - \sigma_{c^{QCD},vis}$$

- EW charm cross section is extrapolated via  $C_{ext} = N_{full}^{EW} / N_{vis}^{EW}$

$$\sigma_{c^{EW}} = C_{ext} \sigma_{c^{EW},vis}$$

$e^+p$	MC Contribution (%)			
	$d \rightarrow c$	$s \rightarrow c$	$\bar{c} \rightarrow \bar{s}(d)$	$g \rightarrow c\bar{c}$
$\sigma_{c,vis}^{MC} + \sigma(g \rightarrow c\bar{c})$	9	45	40	6
$\sigma_{c^{EW}}^{MC} + \sigma(g \rightarrow c\bar{c})$	7	31	58	4
$e^-p$	MC Contribution (%)			
	$\bar{d} \rightarrow \bar{c}$	$\bar{s} \rightarrow \bar{c}$	$c \rightarrow s(d)$	$g \rightarrow c\bar{c}$
$\sigma_{c,vis}^{MC} + \sigma(g \rightarrow c\bar{c})$	3	45	40	12
$\sigma_{c^{EW}}^{MC} + \sigma(g \rightarrow c\bar{c})$	2	31	57	10

# Charm cross section

- Visible charm cross section

$$\sigma_{c,vis} = \frac{N^{data} - N_{bg}^{MC}}{N_c^{MC}} * \sigma_c^{MC}$$

$$= \frac{N^{data} - N_{bg}^{MC}}{N_c^{MC}} * \frac{N_{vis}}{L}$$

- Visible EW charm cross section is not measured. Instead, the QCD part is taken as a systematic.

- EW charm cross section is extrapolated via  $C_{ext} = N_{full}^{EW} / N_{vis}^{EW}$

$$\sigma_{c^{EW}} = C_{ext} \sigma_{c,vis}$$

$e^+p$	MC Contribution (%)			
	$d \rightarrow c$	$s \rightarrow c$	$\bar{c} \rightarrow \bar{s}(\bar{d})$	$g \rightarrow c\bar{c}$
$\sigma_{c,vis}^{MC} + \sigma(g \rightarrow c\bar{c})$	9	45	40	6
$\sigma_{c^{EW}}^{MC} + \sigma(g \rightarrow c\bar{c})$	7	31	58	4
$e^-p$	MC Contribution (%)			
	$\bar{d} \rightarrow \bar{c}$	$\bar{s} \rightarrow \bar{c}$	$c \rightarrow s(d)$	$g \rightarrow c\bar{c}$
$\sigma_{c,vis}^{MC} + \sigma(g \rightarrow c\bar{c})$	3	45	40	12
$\sigma_{c^{EW}}^{MC} + \sigma(g \rightarrow c\bar{c})$	2	31	57	10

ARIADNE predicts QCD part to be small. But, the QCD calculation here is cannot be considered reliable.



# Charm cross section

- Visible charm cross section

$$\sigma_{c,vis} = \frac{N^{data} - N_{bg}^{MC}}{N_c^{MC}} * \sigma_c^{MC}$$

$$= \frac{N^{data} - N_{bg}^{MC}}{N_c^{MC}} * \frac{N_{vis}}{L}$$

- Visible EW charm cross section is not measured. Instead, the QCD part is taken as a systematic.

- EW charm cross section is extrapolated via  $C_{ext} = N_{full}^{EW} / N_{vis}^{EW}$

$$\sigma_{c^{EW}} = C_{ext} \sigma_{c,vis}$$

$e^+p$	MC Contribution (%)			
	$d \rightarrow c$	$s \rightarrow c$	$\bar{c} \rightarrow \bar{s}(d)$	$g \rightarrow c\bar{c}$
$\sigma_{c,vis}^{MC} + \sigma(g \rightarrow c\bar{c})$	9	45	40	6
$\sigma_{c^{EW}}^{MC} + \sigma(g \rightarrow c\bar{c})$	7	31	58	4
$e^-p$	MC Contribution (%)			
	$\bar{d} \rightarrow \bar{c}$	$\bar{s} \rightarrow \bar{c}$	$c \rightarrow s(d)$	$g \rightarrow c\bar{c}$
$\sigma_{c,vis}^{MC} + \sigma(g \rightarrow c\bar{c})$	3	45	40	12
$\sigma_{c^{EW}}^{MC} + \sigma(g \rightarrow c\bar{c})$	2	31	57	10

- Higher contribution from strange-sensitive QPM process in the visible range.

# Systematic uncertainties

## $\delta_1$ Vertex rescaling

- More secondary vertex in MC. For the nominal result, a rescaling is applied for both  $N_c$  and  $N_{bg}$ . For systematic, this was only applied on  $N_{bg}$ .

## $\delta_2$ EW charm fraction

- QCD contribution to MC charm signal is taken as a systematic uncertainty.

## $\delta_3$ LF background

- Uncertainty associated with remaining LF background was estimated by varying  $N_{bg}$  by  $\pm 30\%$ .

## $\delta_4$ CC DIS selection

- Taken from previous ZEUS analysis. (arXiv:1008.3493)

## $\delta_5$ Jet energy scale

- Uncertainty associated with calorimeter is  $\sim 3\%$ . Measurement was repeated with  $E_T$  cut varied by  $\sim 3\%$  in the MC.

## $\delta_6$ Luminosity (**Not included**)

- Uncertainty in ZEUS luminosity measurement is  $\sim 2\%$ .

## $\delta_7$ Signal extraction method & secvtx selection (**Not included**)

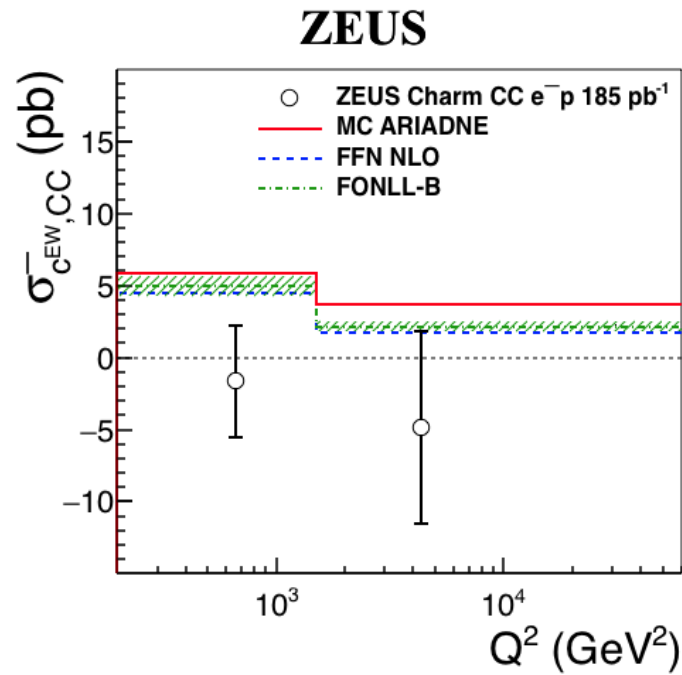
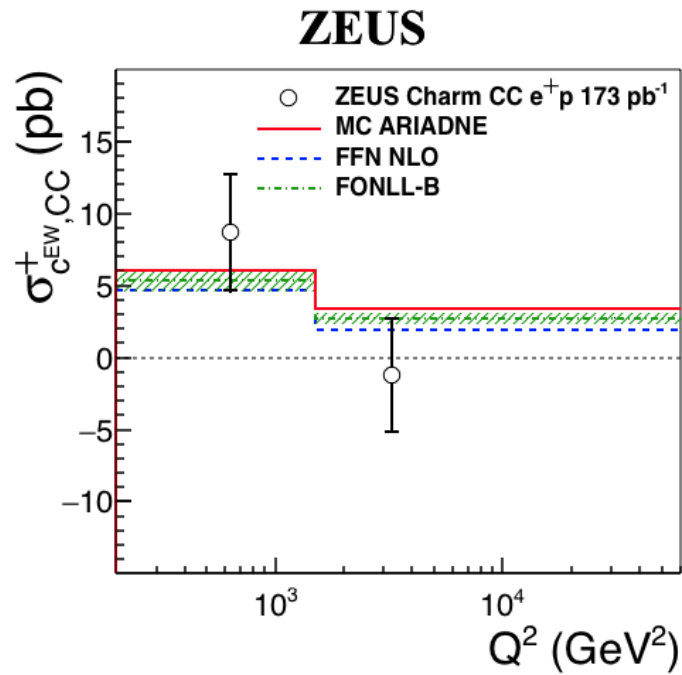
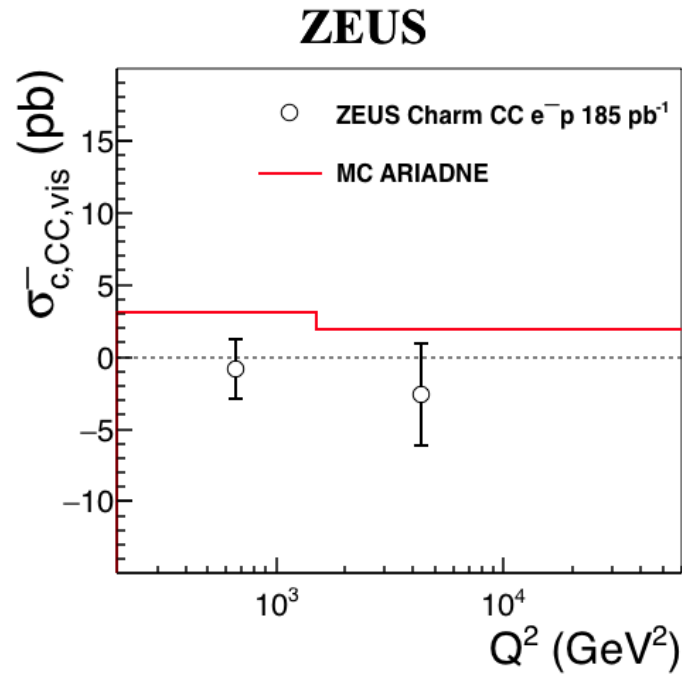
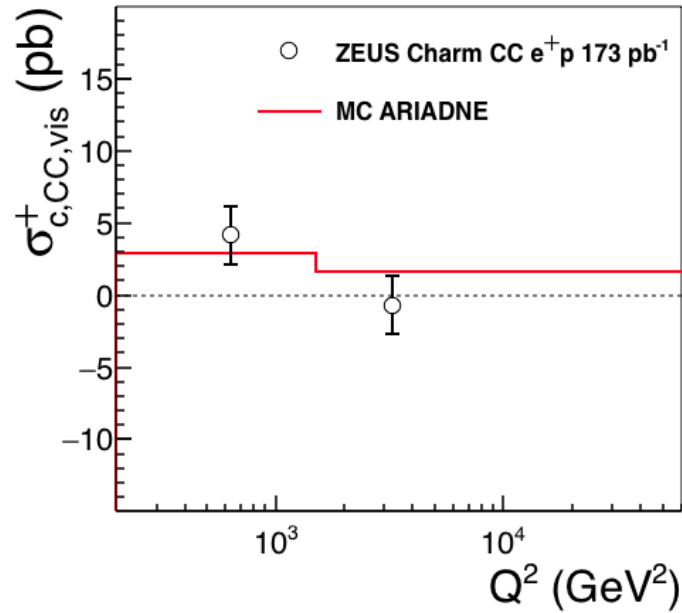
- This could only be tested with the low statistics available at the cross section stage and was not included in the final number. It could be as large as  $\pm 6 pb$ .

Sources	$\delta\sigma_{cEW}^+ (pb)$	$\delta\sigma_{cEW}^- (pb)$
Rescaling	-1.2	+0.9
QCD charm fraction	-0.6	-1.1
LF background	$\pm 0.1$	$\pm 0.3$
DIS selection	$\pm 0.2$	$\pm 0.1$
Calorimeter	$\pm 0.0$	$\pm 0.1$
Total	+0.2	+1.0
	-1.3	-1.2

- In MC,  $\sigma_{cEW} \sim 9 pb$



# Results ZEUS



- EW charm production in CCDIS is measured with HERA II data.
  - Consistent with theory predictions, although statistically limited.

# Re

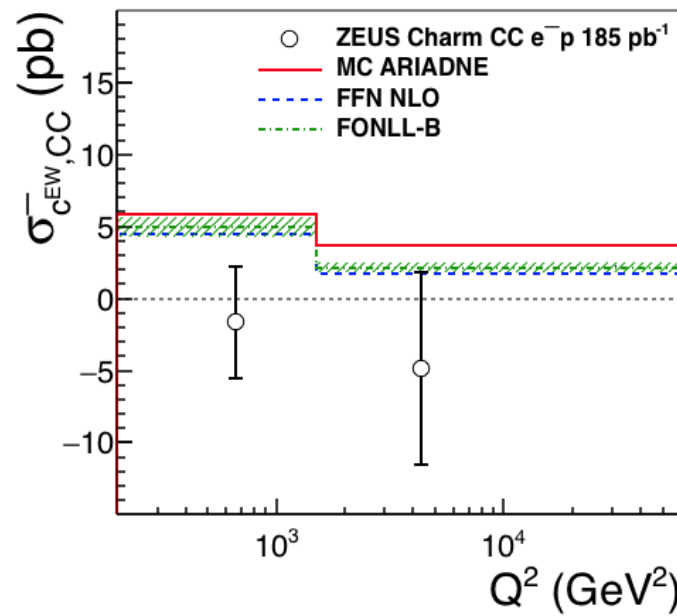
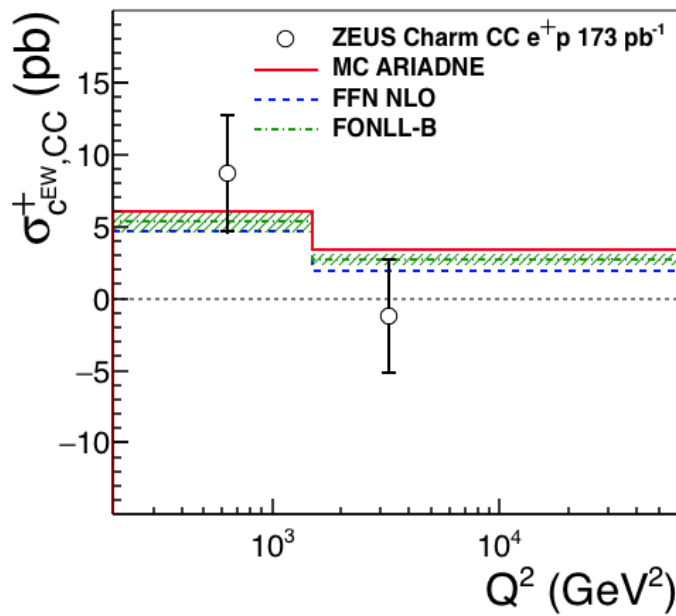
$e^+p$	Contribution (%)					
	$200 < Q^2 < 1500 \text{ GeV}^2$			$1500 < Q^2 < 60000 \text{ GeV}^2$		
	$d \rightarrow c$	$s \rightarrow c$	$\bar{c} \rightarrow \bar{s}(\bar{d})$	$d \rightarrow c$	$s \rightarrow c$	$\bar{c} \rightarrow \bar{s}(\bar{d})$
ARIADNE MC	6	36	58	10	26	64
FFN NLO ABMP16.3	8	49	43	16	43	41
FONLL-B NNPDF3.1	8	43	40	12	37	51

$e^-p$	Contribution (%)					
	$200 < Q^2 < 1500 \text{ GeV}^2$			$1500 < Q^2 < 60000 \text{ GeV}^2$		
	$\bar{d} \rightarrow \bar{c}$	$\bar{s} \rightarrow \bar{c}$	$c \rightarrow s/d$	$\bar{d} \rightarrow \bar{c}$	$\bar{s} \rightarrow \bar{c}$	$c \rightarrow s/d$
ARIADNE MC	3	37	60	2	29	69
FFN NLO ABMP16.3	4	51	45	5	49	46
FONLL-B NNPDF3.1	4	43	53	4	33	63

**ZEUS**

**ZEUS**



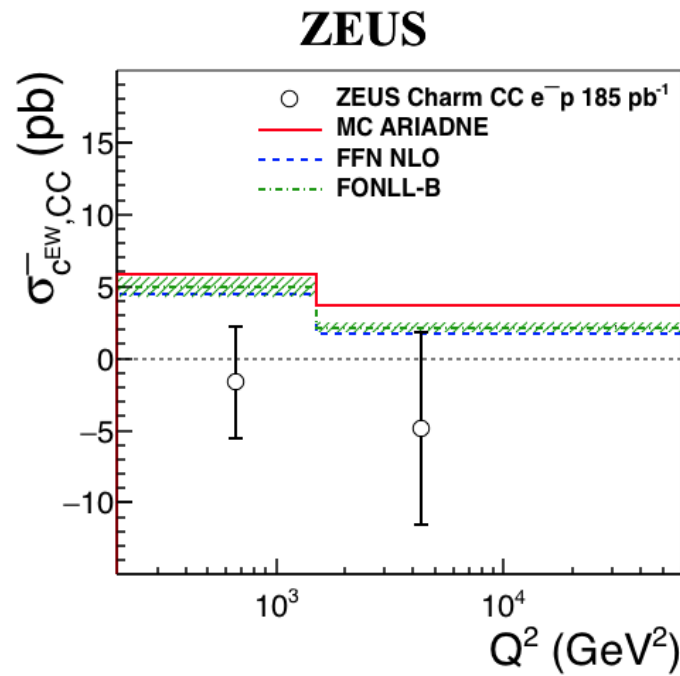
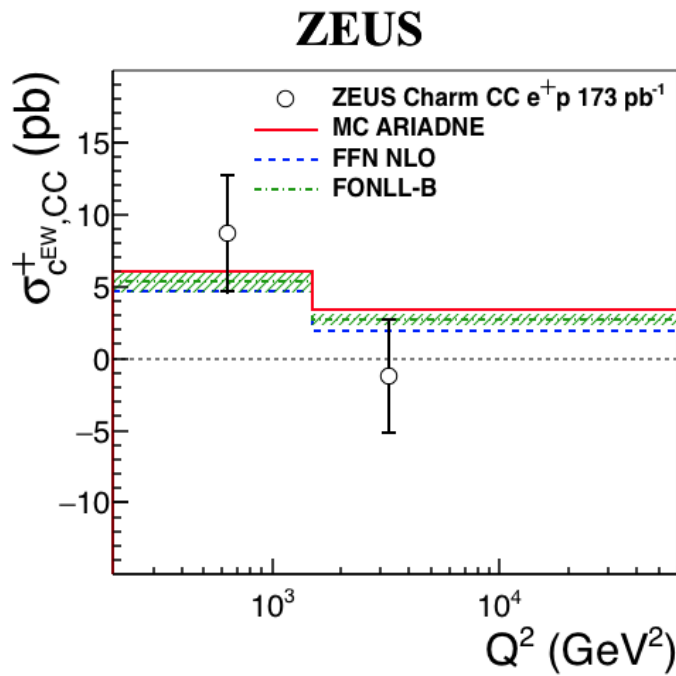
- EW charm production in CCDIS is measured with HERA II data.
  - Consistent with theory predictions, although statistically limited.
  - About the same contribution shared between QPM-like and BGF-like processes. Varies between different theory models.

# Results

$Q^2$ range (GeV <sup>2</sup> )	NLO Predictions (pb)					
	HERAPDF2.0					ATLAS- <i>epWZ16</i>
	$f_s = 0.4$ (nominal)	$f_s = 0.3$	$f_s = 0.5$	$f'_s =$ HERMES <sup>-</sup>	$f'_s =$ HERMES <sup>+</sup>	
$e^+p$						
200 – 1500	5.67	5.40	5.96	5.05	5.38	6.41
1500–60000	2.57	2.47	2.65	2.16	2.20	3.07
$e^-p$						
200 – 1500	5.41	5.15	5.70	4.79	5.12	6.14
1500–60000	2.30	2.21	2.37	1.89	1.93	2.78

EW charm production in CCDIS is measured with HERA II data.

- Consistent with theory predictions, although statistically limited.
  - About the same contribution shared between QPM-like and BGF-like processes. Varies between different theory models.
  - Different assumptions on the strangeness in the proton results in  $\Delta\sigma_{cEW} \sim 1 \text{ pb}$ .
- ~ 2 orders of magnitude higher statistics to be decisive.



# Results

$Q^2$ range (GeV <sup>2</sup> )	NLO Predictions (pb)					
	HERAPDF2.0					ATLAS- <i>epWZ16</i>
	$f_s = 0.4$ (nominal)	$f_s = 0.3$	$f_s = 0.5$	$f'_s =$ HERMES <sup>-</sup>	$f'_s =$ HERMES <sup>+</sup>	
$e^+p$						
200 – 1500	5.67	5.40	5.96	5.05	5.38	6.41
1500–60000	2.57	2.47	2.65	2.16	2.20	3.07
$e^-p$						
200 – 1500	5.41	5.15	5.70	4.79	5.12	6.14
1500–60000	2.30	2.21	2.37	1.89	1.93	2.78

EW charm production in CCDIS is measured with HERA II data.

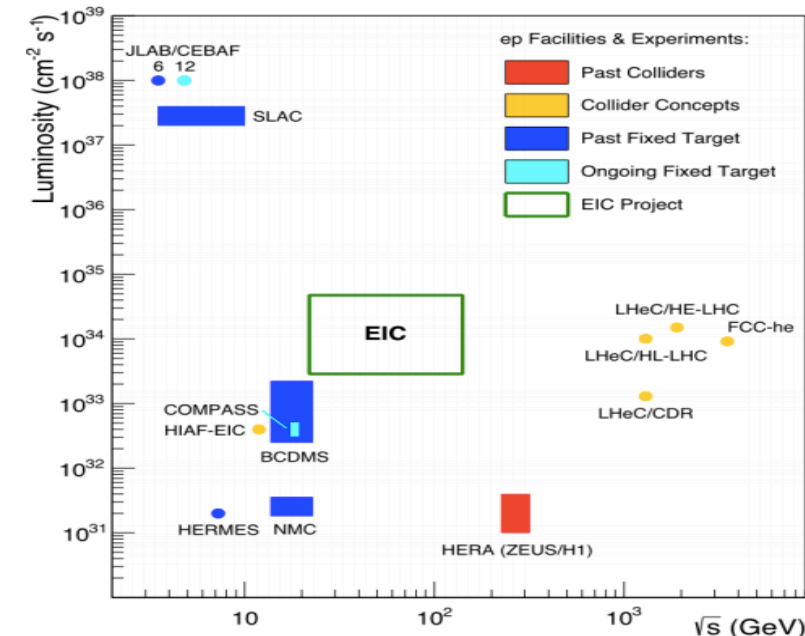
- Consistent with theory predictions, although statistically limited.
- About the same contribution shared between QPM-like and BGF-like processes. Varies between different theory models.
- Different assumptions on the strangeness in the proton results in  $\Delta\sigma_{cEW} \sim 1 pb$ .  
→ ~ 2 orders of magnitude higher statistics to be decisive.
- The uncertainty in the theory predictions  $\delta\sigma_{cEW} \sim 1 pb$ .  
→ some improvements in theory needed.

$Q^2$ range (GeV <sup>2</sup> )	NLO Predictions (pb)							
	FFN ABMP16.3				FONLL-B NNPDF3.1			
	$\sigma$	uncertainties			$\sigma$	uncertainties		
		PDF	scale	mass		PDF	scale	mass
$e^+p$								
200 – 1500	4.72	±0.05	+0.31 -0.23	±0.02	5.37	±0.21	+0.68 -0.73	±0.00
1500–60000	1.97	±0.03	+0.18 -0.13	±0.01	2.66	±0.23	+0.37 -0.26	±0.00
$e^-p$								
200 – 1500	4.50	±0.05	+0.31 -0.23	±0.02	4.98	±0.22	+0.66 -0.71	±0.00
1500–60000	1.73	±0.03	+0.18 -0.13	±0.01	2.16	±0.22	+0.33 -0.21	±0.00



# Summary & Outlook

- EW charm production in high- $Q^2$   $e^\pm p$  CCDIS at HERA has been measured for the first time.
  - Consistent with theory predictions, although statistically limited.
  - Manageable systematic uncertainties.
  - Higher contribution from strange-sensitive process in the visible kinematic region than in the full range.
- Theory predictions with different assumptions of the strangeness in the proton.
  - $\sim 2$  orders of magnitude higher statistics required to investigate the strangeness in the proton, which could be achieved by higher luminosity & better vertex detection resolution in future colliders.
  - Some improvements in theory calculations.
- Potential of DIS has been tested.
  - Better understanding of the strangeness in the proton expected in future lepton-ion collider experiments, such as EIC in the U.S., LHeC at CERN, and EicC in China.



# Backup

$Q^2$ range (GeV <sup>2</sup> )	$\sigma_{c,\text{vis}}$ (pb)				$\sigma_{c^{\text{EW}}}$ (pb)					
$e^+p$										
200–1500	4.1	$\pm 2.0$	(stat.)	$^{+0.1}_{-0.6}$	(syst.)	8.7	$\pm 4.1$	(stat.)	$^{+0.2}_{-1.4}$	(syst.)
1500–60000	-0.7	$\pm 2.0$	(stat.)	$^{+0.2}_{-0.0}$	(syst.)	-1.2	$\pm 3.9$	(stat.)	$^{+0.3}_{-0.3}$	(syst.)
$e^-p$										
200–1500	-0.9	$\pm 2.1$	(stat.)	$^{+0.2}_{-0.0}$	(syst.)	-1.7	$\pm 3.9$	(stat.)	$^{+0.3}_{-0.3}$	(syst.)
1500–60000	-2.6	$\pm 3.5$	(stat.)	$^{+0.5}_{-0.1}$	(syst.)	-4.8	$\pm 6.7$	(stat.)	$^{+0.9}_{-0.8}$	(syst.)

$$\sigma_{c,\text{vis}}^+ = 4.0 \pm 2.8 \text{ (stat.) } ^{+0.1}_{-0.6} \text{ (syst.) pb,}$$

$$\sigma_{c^{\text{EW}}}^+ = 8.5 \pm 5.5 \text{ (stat.) } ^{+0.2}_{-1.3} \text{ (syst.) pb,}$$

$$\sigma_{c,\text{vis}}^- = -3.0 \pm 3.8 \text{ (stat.) } ^{+0.5}_{-0.1} \text{ (syst.) pb,}$$

$$\sigma_{c^{\text{EW}}}^- = -5.7 \pm 7.2 \text{ (stat.) } ^{+1.0}_{-1.2} \text{ (syst.) pb.}$$





